

Energy & Environmental Science

Accepted Manuscript



This is an *Accepted Manuscript*, which has been through the Royal Society of Chemistry peer review process and has been accepted for publication.

Accepted Manuscripts are published online shortly after acceptance, before technical editing, formatting and proof reading. Using this free service, authors can make their results available to the community, in citable form, before we publish the edited article. We will replace this *Accepted Manuscript* with the edited and formatted *Advance Article* as soon as it is available.

You can find more information about *Accepted Manuscripts* in the [Information for Authors](#).

Please note that technical editing may introduce minor changes to the text and/or graphics, which may alter content. The journal's standard [Terms & Conditions](#) and the [Ethical guidelines](#) still apply. In no event shall the Royal Society of Chemistry be held responsible for any errors or omissions in this *Accepted Manuscript* or any consequences arising from the use of any information it contains.

Organic photoelectrochemical cells with quantitative photocarrier conversion

Antonio Guerrero,¹ Marta Haro,¹ Sebastiano Bellani,² Maria Rosa Antognazza,²
Laura Meda,³ Sixto Gimenez,^{*1} Juan Bisquert^{*1,4}

¹ Photovoltaics and Optoelectronic Devices Group, Departament de Física, Universitat Jaume I, 12071 Castello, Spain

² Center for Nano Science and Technology @Polimi, Istituto Italiano di Tecnologia, Via Pascoli 70/3, 20133 Milano, Italy

³ ENI-Donegani Institute, Research Center for Non-Conventional Energies Via Fauser 4, 28100 Novara, Italy

⁴ Department of Chemistry, Faculty of Science, King Abdulaziz University, Jeddah, Saudi Arabia

Corresponding authors Email: sjulia@uji.es, bisquert@uji.es

9 June 2014

Abstract

Efficient solar-to-fuel conversion could be a cost-effective way to power the planet with sunlight. Herein, we demonstrate that Organic Photoelectrochemical Cells (OPEC) constitute a versatile platform for the efficient production of solar fuels production. We show that the photogenerated carriers at the organic active layer can be quantitatively extracted to drive photoelectrochemical reactions at the interface with a liquid solution. Indeed, an unprecedented photocurrent of $4 \text{ mA} \cdot \text{cm}^{-2}$ is extracted for an OPEC device, comparable to that of a solid-state device with similar optical properties. By a careful choice of the selective contact and the redox couple in the liquid medium, we can tune the energetics of the system and activate either oxidative or reductive chemistry. The design rules to drive the desired electrochemical reaction are provided based on a comprehensive study of the energetic aspects of the OPEC configuration. Finally, we demonstrate that OPEC devices effectively produce hydrogen in acetonitrile when a cobaloxime based homogeneous catalyst is present in the solution, and HCl is used a source of protons.

Introduction

Converting the energy of solar photons into chemical bonds is termed solar fuel production. This is the purpose of photoelectrochemical cells (PEC) that aim to convert abundant compounds dissolved in liquid medium into a useful fuel by electrochemical reactions powered only by solar photons.¹ Reduction of CO₂ by similar means is also of great interest for environmental purposes. The realization of a cost-effective device would bring a major step towards reliable renewable energy economy, but it has not been achieved yet. Recently, the quest of semiconductors that fulfils properties of light absorption, charge separation, and adequate energy levels for realizing the required photoelectrochemical reactions in combination with suitable surface catalysts, has driven a great research effort. However, so far the mainstream of research in materials and processes involves either metal oxide inorganic semiconductors such as TiO₂,² Fe₂O₃,³ WO₃⁴ and BiVO₄⁵ or conventional photovoltaic materials as Si and CuIn_{1-x}Ga_xSe₂ (CIGS).⁶

Meanwhile, organic photovoltaic materials have experienced extraordinary development with a great potential to produce inexpensive devices. Organic bulk heterojunction (BHJ) operation is based on ultrafast transference of carriers from an absorbing polymer or small organic molecule to a functionalized fullerene.⁷ Intermediate efficiency BHJ cells, such as the archetypal combination poly(3-hexylthiophene):[6,6]-phenyl C₆₁-butyric acid methyl ester (P3HT:PCBM) can provide up to $\approx 10 \text{ mA cm}^{-2}$ photocurrent, 0.63 V open circuit voltage, and high fill factor using a standard configuration. A careful combination of factors in the latest generation devices, such as optimization of donor-acceptor blend morphology, synthesis of low bandgap molecules that show increased light absorption, and improvement of transport properties and selective contacts, has provided large efficiencies of solar to electricity

conversion around 10%.^{8,9} The progress of organic cells demonstrates the versatility of organic photovoltaic materials, which can be designed and improved to realize highly efficient devices.

Despite these developments, the application of photoactive organic materials for solar fuel production has been marginally explored. The use of BHJ blend materials in solar fuel production requires that two fundamental conditions are satisfied: (i) the organic blend must preserve the capability of generating charges even when it is in direct contact with a liquid electrolyte; (ii) the photovoltage must be high enough in order to allow efficient charge transfer between the organic film and the electrolyte. The coupling of photogeneration in organic conductors and blends with liquid electrolytes has been investigated for a long time,¹⁰⁻¹⁵ but the obtained photocurrents have been significantly lower compared to those expected from the light harvesting efficiency, evaluated through optical absorbance measurements. Additionally, the mechanisms leading to gas evolution remain controversial. Consequently, a detailed understanding of the interfacial processes is urgently needed, in order to fill the gap between the theoretically achievable photocurrent (on the base of conventional organic solar cells) and practical results obtained with photoelectrochemical cells.^{10, 16-18}

The PEC conversion requires the combination of three factors. In first place, the photovoltaic material in contact with a liquid medium must function efficiently in terms of light absorption, internal charge separation, and transport to the active surface. Second, the band edge positions should be appropriately located to allow electron (hole) transfer to the solution to be reduced (oxidised). The third step involves that the interfacial charge transfer must occur at significant pace when the surface is contacted with the relevant compound to be transformed into a fuel, e.g., water or CO₂. This last issue may require the assistance of a catalyst that facilitates the given electrochemical

reaction. Unfortunately, up to date these factors have not been comprehensively studied in an Organic Photoelectrochemical Cell (OPEC) configuration.

In summary, it is first necessary to demonstrate that the BHJ photovoltaic blend operates efficiently when the liquid medium replaces one of the metal contacts of the solar cell. In this paper we address this question and we show high current and voltage of standard P3HT:PCBM blends contacted by different electrolytes. We investigate the internal processes of photon-to-carrier conversion at the organic/liquid interface and we show inversion of current depending on the nature of contacts and redox couple. Furthermore, we demonstrate photocurrents of hydrogen generation of $1 \text{ mA} \cdot \text{cm}^{-2}$ when cobaloxime based catalysts are introduced in the solution. This study demonstrates the high potential of OPEC for solar fuel production.

Results and discussion

The first step in our study is to understand if there is a fundamental limitation in the photogeneration and charge extraction of carriers when a liquid electrolyte is in contact with the organic active layer. With this objective in mind, we prepared devices mimicking those known to work efficiently as BHJ solar cells (Figure 1a). In this configuration ZnO and MoO₃ act as interfacial layers (IFL) selective to electrons and holes, respectively. Fig. 1(c) shows the current density-voltage characteristics of representative organic BHJ solar cells with the structure ITO/ZnO/P3HT:PCBM/MoO₃/Ag. These cells show the standard electrical characteristics for this type of device widely reported in the literature.¹⁹ When a thick layer of silver (100 nm) is used, the back contact acts as a mirror, reflecting some of the incident light, and increasing the effective incident path length. On the other hand, when a thin layer of silver (20 nm) is used, the device is semitransparent and the light

harvesting at the active layer is decreased, explaining the lower photocurrent observed.

In the OPEC configuration the absorber layer is contacted by a liquid electrolyte and the result of the photocurrent is to drive a interfacial reaction at the solid/liquid contact. Ultimately such reaction must provide a useful fuel, however in the present study we first focus the study on facile electrochemical reactions that show the operation of the photoactive organic blend in contact with a liquid medium.

Thus the hole selective layer, MoO_3 , was replaced by a redox couple able to accept holes from the active organic electrode in an organic solvent with a large electrochemical window (Figure 1b). In particular, an acetonitrile solution is used containing Ferrocene/Ferrocene⁺ (Fc/Fc^+) as redox couple and tetrabutyl ammonium hexafluorophosphate ($\text{N}(\text{Bu}^n)_4\text{PF}_6$) as support electrolyte. When the MoO_3/Ag contact is replaced by the Fc/Fc^+ redox couple in the OPEC configuration with a Pt counterelectrode, a sizeable photocurrent of 4 mA cm^{-2} is observed, which is to the best of the authors' knowledge, the highest current reported in an all-organic PEC device. Interestingly, both semitransparent BHJ and OPEC show similar photoconversion properties as reflected by the external quantum efficiencies (EQE) in Fig. 1(d). In addition, when the OPEC device is illuminated through the electrolyte, the photocurrent drops to about 1 mA/cm^2 due to the optical losses at the cell chamber. All these results clearly indicate that the OPEC device realizes quantitative carrier extraction to the electrolyte comparable to that of an optimized metal contact. An improvement of the optical engineering of the device may lead to enhanced photocurrents.

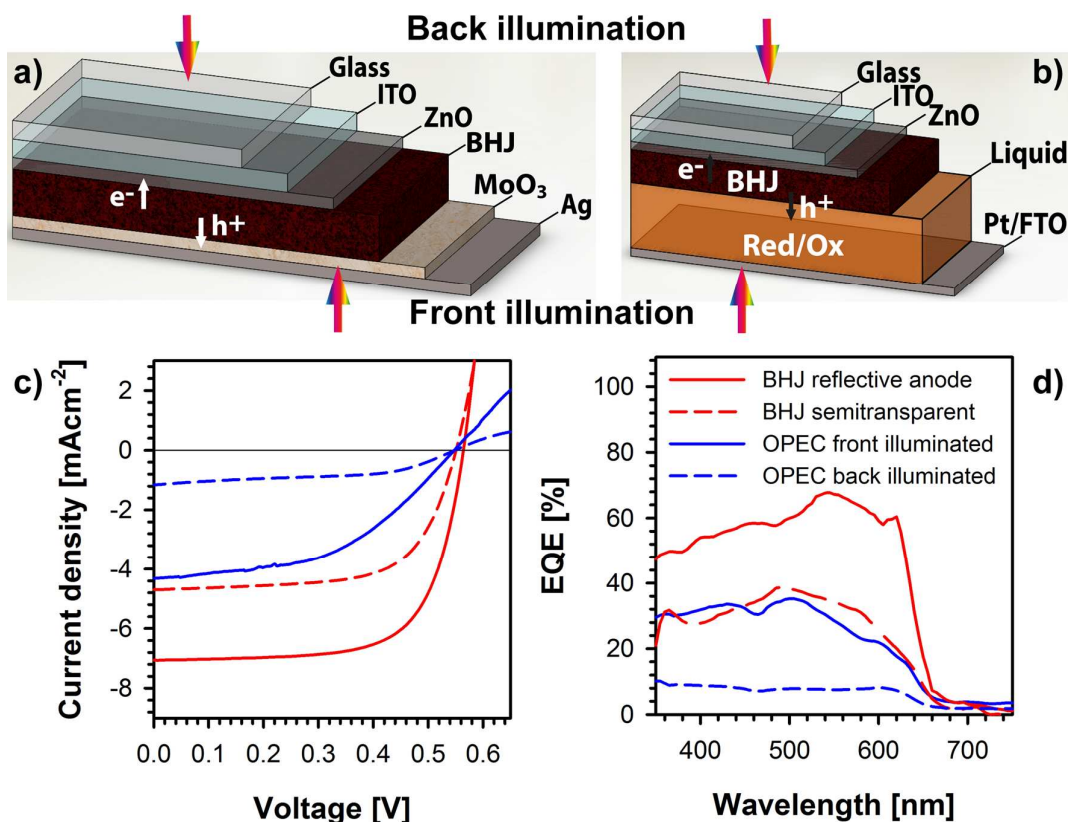


Figure 1: (a) Device architecture of a BHJ solar cell and (b) Organic Photoelectrochemical Cell (OPEC). The illumination direction for both devices is indicated. The main difference in the OPEC configuration is the presence of a liquid solution with a redox couple able to extract carriers to the solution. (c) Current density/voltage characteristic and (d) External Quantum Efficiency (EQE) of devices fabricated in both configurations. Reflective and semi-transparent BHJ refer to devices with 100 nm and 20 nm thick Ag layer, respectively.

The rational design in an OPEC cell able to transform the incoming solar energy into chemical energy entails the adequate selection of the interfacial layer (IFL) and redox couple: this would allow efficient extraction of electrons or holes to the electrolyte solution through specific chemical reaction. For this purpose, two interfaces should be considered, both the IFL/organic blend and the organic blend/electrolyte interfaces. The first one has been intensively studied in organic photovoltaic devices since the energy level equilibration at the contacts determines the confinement of the electrical field

providing efficient collection of carriers.²⁰⁻²³ Furthermore, considering other kind of photoelectrochemical cells (based on colloidal quantum dots), it has been recently demonstrated that the selection of an adequate IFL can determine the sign of the photovoltage, i.e. the direction of the photogenerated charges (electrons and holes) that are driven to the collector and to the solution.²⁴ With these results in mind, we have selected a hole (ZnO) and an electron (PEDOT:PSS) blocking layers as IFL in our OPEC devices. For the selection of the redox couples, Marcus theory^{25, 26} has been considered and Fc/Fc⁺ redox potential (4.9 eV) matches well with the HOMO level of the polymer (5.0 eV) and BZQ/BZQ⁻ (with a redox potential 4.0 eV close to the LUMO of the fullerene, 3.2 eV). Consequently, both systems, Fc/Fc⁺ and BZQ/BZQ⁻ have been selected as hole and electron acceptors, respectively.

In order to elucidate whether the organic active layer is able to photogenerate similar charge density in both PV and OPEC configurations, continuous-wave photoinduced absorption (CW-PIA) spectroscopy experiments were carried out. CW-PIA monitors the change in the transmission spectrum of the organic active layer due to the absorption of long-lived (>10 μ s) charged states. Hence, P3HT provides a spectroscopic fingerprint, which allows quantifying the occurrence of polarons in the presence of a redox electrolyte in contact with the organic blend. Polarons are localized defects generated by an introduced charge carrier –electron or hole- into a polymer together with the consequent polarization locally centered on the charge.²⁷ These polarons have associated energy quantum states, which are responsible for the CW-PIA spectra. Figure 2 shows representative “in-phase” and “out-of-phase” CW-PIA spectra of the ITO/ZnO/BHJ and ITO/PEDOT:PSS/BHJ systems in air. The excited state photophysics of the P3HT/PCBM blend has been extensively studied in air, allowing the identification of the broad absorption feature between 620-1100 nm as due to two overlapping polaron

absorption bands, peaking at 780 nm (free polarons) and at 960 nm (localized polarons).²⁸ Figure 2a shows that, when the electrode ITO/ZnO/BHJ is immersed into an electrolyte solution containing the Fc/Fc⁺ redox couple, the polaronic fingerprint of P3HT matches the signal obtained in air, suggesting that charge generation within the organic BHJ is not altered by the presence of the liquid electrolyte. Similar results have been previously obtained in PPV-based polymers in contact with aqueous electrolytes, focusing however on much shorter timescales, relevant for charge generation processes.²⁹ On the other hand, when the ITO/PEDOT:PSS/BHJ system is immersed into the BZQ/BZQ⁻ solution (Figure 2b), the broad signal in the in-phase spectrum increases compared to that obtained in air and a clear response is observed in the out-of-phase spectrum (assigned to the absorption of very long-lived species). These two differences suggest longer photogenerated carrier lifetimes and can be ascribed to the presence of surface states.^{30, 31} However, other causes that can increase the lifetime of the photogenerated charges cannot be excluded, namely, a photoactivated doping that leads to more hydrophilic surfaces that changes the electrostatic interactions, or else screening of the electric field probably due to a different orientation of the chains.³²

CW-PIA measurements of the systems immersed into the electrolyte solutions were repeated after 20 minutes, with identical results, indicating that no degradation phenomena affecting the photogeneration of charges in the organic blend take place within this time scale. This result is in good agreement with the stability test described below. All in all, these results suggest that the presence of a liquid electrolyte containing a redox couple does not significantly affect the photogeneration process in the active layer BHJ, increasing the polaron lifetime when BZQ/BZQ⁻ acts as an electron scavenger.

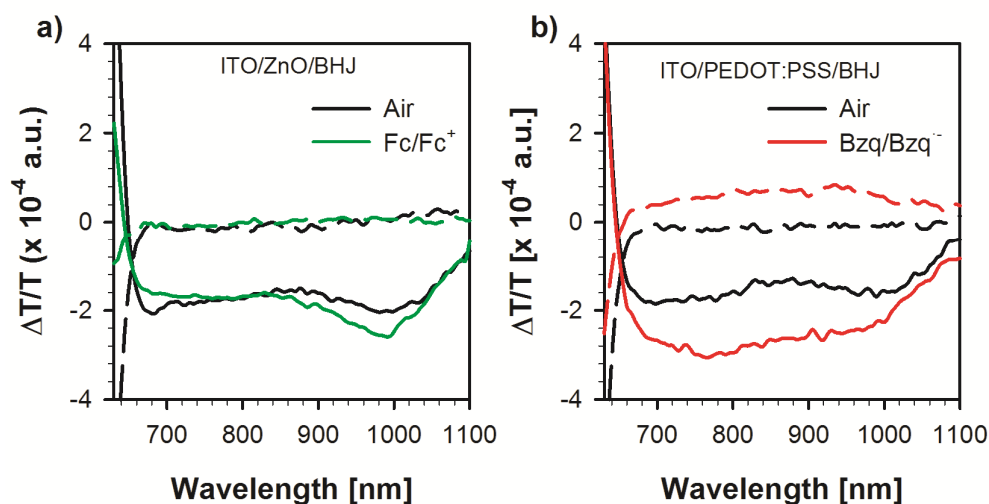


Figure 2: Continuous-wave photo-induced absorption spectra of (a) ITO/ZnO/BHJ and (b) ITO/PEDOT:PSS/BHJ in air and in the presence of Fc-Fc⁺ and BZQ-BZQ⁻ redox couples, respectively. Solid lines correspond to in-phase response and dashed lines to out-of-phase response. Optical excitation at 561 nm, modulation frequency of 133 Hz.

The energetic aspects of the OPEC system have been studied using a three-electrode configuration, with Ag/Ag⁺ reference electrode, a graphite rod as counter-electrode and the system under study as working electrode. Figure 3 shows the j - V plots under chopped illumination for the designed systems to inject holes and electrons to the solution, ITO/ZnO/BHJ/Fc-Fc⁺ and ITO/PEDOT:PSS/BHJ/BZQ-BZQ⁻, respectively (additional ITO/IFL/redox couple combinations are shown and discussed in the Supplementary Information, Supplementary Figure S1). Figure 3a shows that the hole photocurrent (positive photocurrent) increases at positive bias indicating holes injected to the solution upon illumination and nearly 4 mA/cm² are achieved at +1V vs Fc-Fc⁺. Moreover, the dark current is low indicating that the electrolyte and redox couple efficiently block the injection of electrons into the solution, as expected for a selective contact. Interestingly, at voltages close to -1V vs Fc-Fc⁺ we observe an inversion of the photocurrent, indicating that electrons are collected by the solution. We show a

magnified area of the region where inversion of the photocurrent takes place as Supplementary Information, S2. This inflexion point is related to the flatband potential V_{fb} , which is the applied potential required to remove pre-existing band-bending at the semiconductor interface. Indeed, this effect of inversion of the photocurrent has been previously observed in lightly doped systems.³³ Similarly, figure 3b shows the increase of the electronic photocurrent (negative photocurrent) in the cathodic sweep indicating the injection of electrons from the system ITO/PEDOT:PSS/BHJ to the BZQ-BZQ⁻ redox couple with practically zero dark current and an turn-on voltage of the photocurrent related to the position of V_{fb} . Again, the obtained photocurrent density is in the order of $\text{mA}\cdot\text{cm}^{-2}$. These results demonstrate that the desired charge carriers can be injected into the electrolyte solution with an adequate selection of both IFL and redox couple. Importantly, OPEC devices based on the configuration ITO/ZnO/BHJ/Fc-Fc⁺ constitute robust and stable devices as evidenced by the chronoamperometry curve obtained during a period of 6 h under shuttered illumination, showed as supporting information (Figure S3). Devices based on the configuration ITO/PEDOT:PSS/BHJ/BZQ-BZQ⁻ were somehow less stable, we are currently investigating the reasons for this degradation.

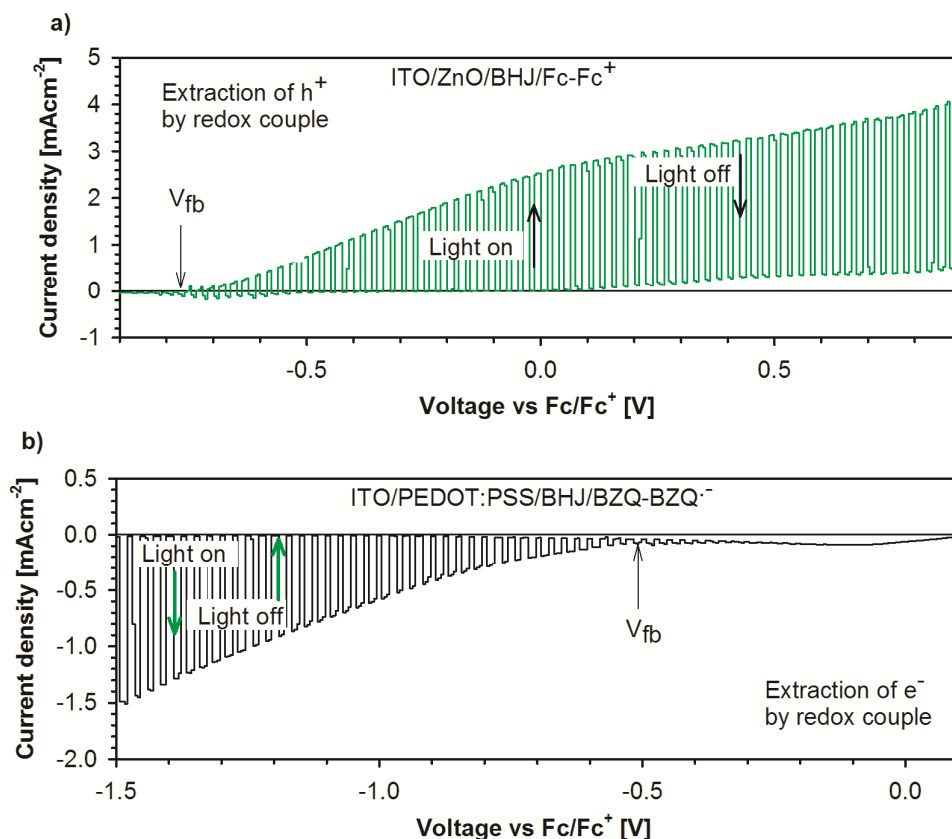


Figure 3: Shuttered J-V curves in acetonitrile (0.1M tetrabutyl hexafluorophosphate) recorded at 5 mV s^{-1} for ITO/PEDOT:PSS/BHJ/Fc-Fc⁺ (a) and ITO/ZnO/BHJ/BZQ-BZQ⁻ (b). The flatband potential (V_{fb}) extracted from Mott-Schottky analysis (see Figure 4) is also indicated. A magnified view of the region where inversion of the photocurrent takes place is shown as Supplementary Information, SI2.

In order to further understand the carrier dynamics of the devices, we performed capacitance-voltage measurements in three-electrode configuration. In these experiments, the working electrode is driven at a DC voltage and a small AC perturbation (1 kHz) is applied, the differential current output is measured and the capacitance is extracted. A single frequency is selected, since the capacitance was observed to be frequency independent in the range of 100 Hz to 10 kHz. Representative Capacitance-Voltage measurements under dark conditions for two OPEC configurations are shown in Figure 4. These results are similar to those typically observed in OPVs: a

constant capacitance that increases at intermediate applied voltages and equilibrates towards positive values. This behaviour is generally observed for p-doped systems and has been previously correlated with the presence of a depleted layer at the organic layer/cathode interface.³⁴ From the Mott-Schottky analysis (C^{-2} versus V) the doping density (n) of the active layer can be extracted. The results for a selection of device configurations are shown as Table 1. Values of n are similar to those previously observed in regular OPVs ($n = 1-10 \times 10^{16} \text{ cm}^{-3}$) indicating that the presence of the liquid solution does not substantially modify the presence of electrically active impurities in the BHJ layer. Note that a different behaviour was observed in contact with aqueous saline electrolytes.³⁵ Although the doping density is related to the properties of the polymer itself, the obtained values are moderately increased by the use of a nano-sized porous ZnO layer that seems to restrict the domain size of the P3HT increasing the values of n .³⁶ In addition, doping values are uncorrelated with the redox couple used during the measurement.

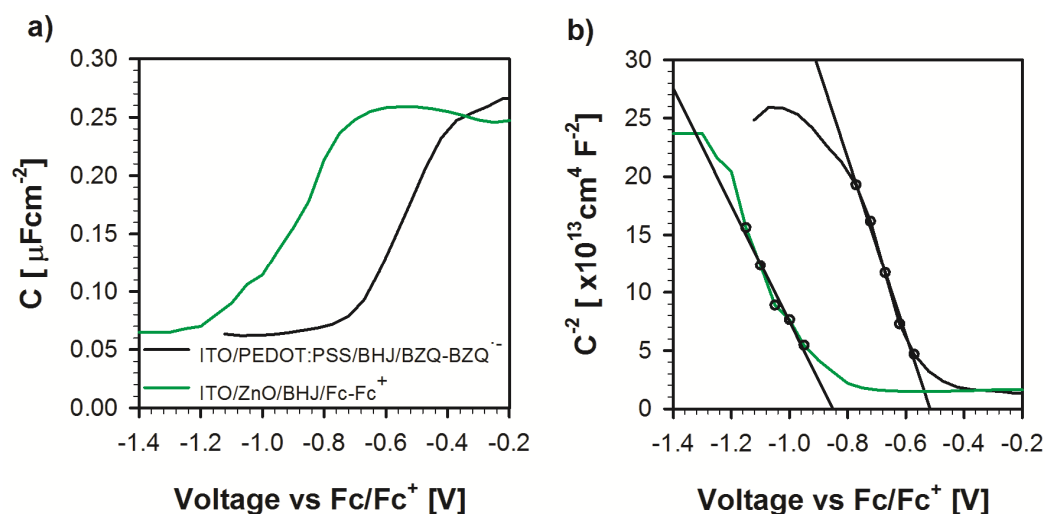


Figure 4: Capacitance-Voltage response (a) and Mott-Schottky analysis (b) of ITO/PEDOT:PSS/BHJ in the presence of BZQ-BZQ⁻ redox couple and ITO/ZnO/BHJ in contact with Fc-Fc⁺ redox couple.

On the other hand, the intercepts of the straight line with the x-axis define the values

of V_{fb} collected in Table 1. At this applied voltage, bands will be flat and collection of carriers at the contacts will not be favoured as carriers will only reach the contacts by diffusion. This explains the very low photocurrent values close to V_{fb} in Figure 3. We note that the values of V_{fb} are strongly dependent on the workfunction of the interfacial layer and the redox potential of the electrolyte solution in good agreement with previous studies.²²

Table 1: Summary of doping density (n) and flat band potential (V_{fb}) extracted from Capacitance-Voltage data for selected OPEC configurations.

IFL	Redox couple	n [$\times 10^{16} \text{ cm}^{-3}$]	V_{fb} [V vs Fc/Fc ⁺]
ZnO	Fc-Fc ⁺	14.1	-0.851
PEDOT:PSS	Fc-Fc ⁺	5.4	-0.490
PEDOT:PSS	BZQ-BZQ ⁻	6.17	-0.516
ZnO	BZQ-BZQ ⁻	38.0	-0.871

Figure 5 depicts the basic elements of the energetic landscape of both optimized OPEC devices (ZnO/BHJ/Fc-Fc⁺ and PEDOT:PSS/BHJ/BZQ-BZQ⁻), showing first the energy levels of the separate materials at constant vacuum level, on top, and the equilibrated junctions at flat Fermi level, on the bottom. The values for the work function of the Fc-Fc⁺ and BZQ-BZQ⁻ redox couples have been obtained by cyclic voltammetry and those for the organic blend, ZnO and PEDOT:PSS have been extracted from literature.^{22, 37, 38} In these diagrams, we have considered a slightly doped organic semiconductor material ($n \sim 10^{16} \text{ cm}^{-3}$), no surface states and a concentration of the redox couple high enough ($>0.1 \text{ M}$) to assume that the potential drop fully takes place

within the semiconductor material at the BHJ/solution interface.³⁹ Figures 5(c) and (d) illustrate the modification of the energy levels after contact equilibration of the system ITO/ZnO/BHJ/Fc-Fc⁺ and PEDOT:PSS/BHJ/BZQ-BZQ⁻, respectively. The working mechanism of BHJ solar cells with ZnO and PEDOT:PSS interfacial layers is well-established.^{40, 41} In those systems the energy levels are well located to drive the photogenerated electrons to the ZnO contact and holes to the PEDOT:PSS. In the OPEC configuration the role of Fc-Fc⁺ is the similar as that of PEDOT:PSS, since they both exhibit similar redox potential and workfunction. We believe that in these conditions the semiconductor is working under accumulation (the Fermi level intercepts the maximum of the valence band). On the other hand, the system ITO/PEDOT:PSS/BHJ/BZQ-BZQ⁻ can drive the photogenerated electrons to the electrolyte solution and the holes to the IFL. These schemes are in good agreement with the photoelectrochemical behavior showed in Figure 3.

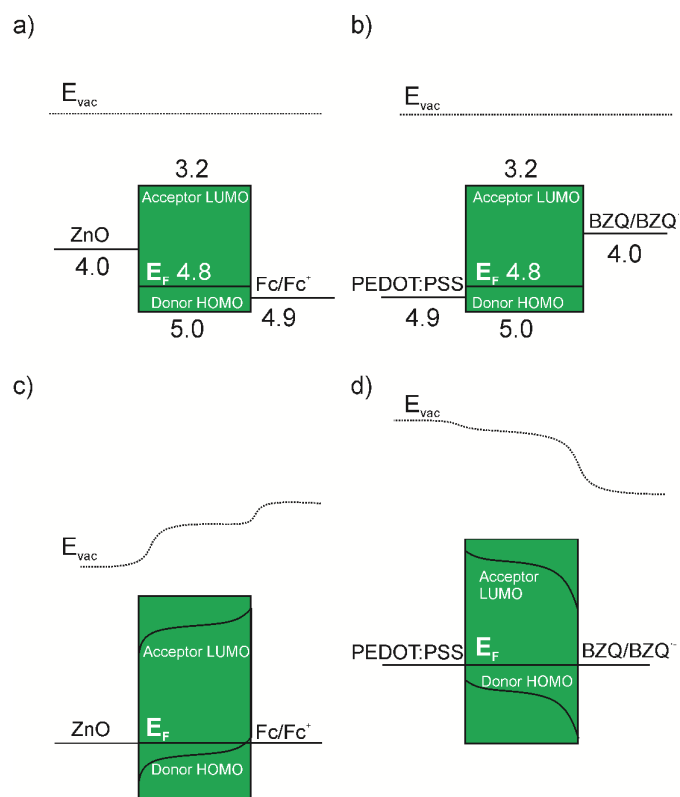


Figure 5: Energy level diagrams representing both high performing OPEC configurations before and after electrical equilibration. The vacuum level is also included. All numbers are referred to eV with respect to the vacuum level (a) ZnO/BHJ/Fc-Fc⁺ before electrical equilibration, (b) PEDOT:PSS/BHJ/BZQ-BZQ⁻ before electrical equilibration, (c) ZnO/BHJ/Fc-Fc⁺ after electrical equilibration, (d) PEDOT:PSS/BHJ/BZQ-BZQ⁻ after electrical equilibration. In (a) and (c) ZnO acts a selective contact for electrons and Fc-Fc⁺ produces a band bending at the BHJ/solution interface enabling the extraction of holes to the solution. In (b) and (d) PEDOT:PSS acts as selective contact for holes and BZQ-BZQ⁻ induces band bending to extract electrons from the organic layer to the solution.

In order to complete our study, we demonstrate solar to fuel energy conversion with an OPEC device. For this purpose, the charge generated in the BHJ electrode is transferred to an homogeneous catalyst (chloro(pyridine)bis(dimethylglyoximate)cobalt III), which is soluble in acetonitrile and replaces the redox couple (benzoquinone). HCl is used as the proton source.

Cobaloximes are cobalt complexes showing powerful nucleophilic behaviour in their reduced state, Co(I). These complexes can be protonated to yield Co(III)-hydride species, which turns into H₂ molecules by either protonation of the hydride moiety or bimolecular reductive elimination.⁴² This behaviour has been exploited to catalyze the hydrogen evolution reaction by electrochemical^{43, 44} or more recently photochemical systems.⁴⁵ Herein, we use for first time these complexes as intermediate catalysts to generate H₂ with the flux of photocarriers provided by an OPEC device.

The photoelectrochemical behaviour of ITO/PEDOT:PSS/BHJ in the presence of the cobaloxime (33 mM) and a proton donor (HCl, 5mM) was first evaluated, Figure 6. The modest HCl concentration guarantees that cobaloxime complexes behave catalytically active.⁴³ In the dark, no current is measured due to the outstanding rectifying properties of the PEDOT:PSS IFL for electrons. Under illumination, the photocurrent follows the typical catalytic wave of cobaloxime complexes in presence of a strong acid; i.e.: the

photocurrent increases with the applied voltage and shows an irreversible peak due to electroreduction of protons, close to the Co(II)/Co(I) reversible wave.^{43, 46} The photocurrent peaks at -0.97 V vs the Fc^+/Fc reference, which corresponds to 3.9 eV with respect to the vacuum level. This value is very close to the redox level of BZQ/BZQ^- (4.0 eV). Consequently, the energetics of the ITO/PEDOT:PSS/BHJ/cobaloxime system is adequate for efficiently driving the photogenerated electrons to the electrolyte solution. Furthermore, the photocurrent maximum (1.15 mA cm^{-2}), is similar to the value obtained when the BZQ/BZQ^- redox couple is used (Figure 3b), as expected in the absence of kinetic barriers. Finally the production of H_2 in the system ITO/PEDOT:PSS/BHJ/cobaloxime was confirmed by labelling experiments. Details of these measurements can be found as Supplementary Information, S4. These results highlight the extraordinary potential of organic semiconductors for the production of solar fuels and validate the developed design rules to provide OPEC systems with tailored electrochemical properties. The ultimate goal is exploiting this configuration in aqueous environments to carry out solar H_2 generation from water splitting and we are intensively working in this direction at our lab.

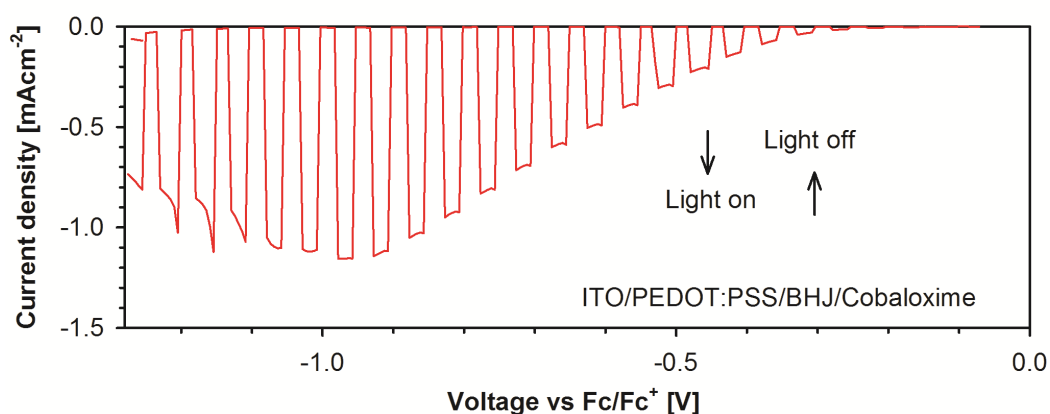


Figure 6. Shuttered J-V curves in acetonitrile (0.1M tetrabutyl hexafluorophosphate) recorded at 5 mV s^{-1} for ITO/PEDOT:PSS/BHJ/cobaloxime and 5 mM in HCl as proton source.

Conclusions

We have demonstrated that organic photoelectrochemical cells (OPECs) are able to quantitatively extract the photocurrent generated in the organic active layer. A record photocurrent of $4 \text{ mA} \cdot \text{cm}^{-2}$ has been obtained for this device, which is to the best of the authors' knowledge the highest photocurrent obtained for an organic photoelectrochemical cell. We have showed that the photogenerated charge at the organic active layer is not affected by the presence of the liquid medium. Moreover, by a careful selection of the redox couple and the interfacial layer, the energetics of the system can be tailored so that the organic blend can provide a flux of either electrons or holes to the solution. Consequently, oxidative or reductive chemistry at the semiconductor/liquid interface can be activated upon demand expanding applicability of the system for the production of different solar fuels. These results can be satisfactorily explained on the basis of energy diagrams, which have been constructed with experimental data and Fermi level alignment. Finally, we demonstrate effective solar to H_2 conversion with an OPEC device coupled to an homogeneous cobaloxime based catalyst. The versatility of organic materials is a solid guarantee for further optimization of OPEC devices, which constitute a real low-cost alternative for the generation of solar fuels.

Methods

Materials

The following materials were used to prepare the OPV and OPEC electrodes: P3HT (Luminescence Technology Corp., MW > 45,000 (GPC)), PC_{60}BM (Solenne, 99.5 %), PEDOT:PSS (CLEVIOS P AI 4083), ZnO (Gene's Ink), MoO_3 (Aldrich, 99.9 %), silver (Aldrich, 99.99 %), ITO (PTB7 labs, $10 \Omega/\text{sq}$), o-dichlorobenzene (Aldrich, 99.9 %). All

materials were used as received without further purification. For OPV fabrication, all manipulations were carried out in a glovebox under a nitrogen atmosphere, unless otherwise stated. P3HT:fullerenes blends were prepared from dry o-dichlorobenzene (1:1, 34 mg/ml) and were stirred at 70 °C for 16 h before sample preparation. For the preparation of the electrolytic solutions acetonitrile (AlfaAesar, 99.8+%), ferrocene (Aldrich, 98.0 %), benzoquinone (Fluka, 99.5 %), and tetrabutyl hexafluorophosphate (Fluka, 99.0 %) were used as received without further purification.

Device fabrication

Organic solar cells (OPVs) were fabricated in the configuration ITO/ZnO/P3HT:PC₆₀BM/MoO₃/Ag, and 25 mm² of active area. Pre-patterned ITO substrates were cleaned and UV-ozone treated. A ZnO nanoparticle solution was spin coated in air at 1000 rpm for 30 seconds followed by thermal treatment at 100 °C for 2 minutes to provide a ZnO layer thickness of ~40 nm. Substrates were transferred to a glovebox equipped with a thermal evaporator and were annealed at 120 °C for 5 minutes. The P3HT: PC₆₀BM layer was deposited at speed of 1200 rpm for 30 seconds and was placed in a petri dish to allow slow drying of the film during a period of 2 h to enable an adequate morphology of the blend. At this point, samples were thermally annealed at 130 °C for 10 min. Evaporation was carried out at a base pressure of 3×10⁻⁶ mbar to provide different thickness of MoO₃/Ag either 7.5/100 nm (reflective anode) or 7.5/15 nm (semitransparent anode). Devices were encapsulated with a photoresin and a glass microscopy slide. Samples were then taken out of the glovebox for device characterization. Similarly, OPEC electrodes in the configuration ITO/ZnO/P3HT:PC₆₀BM were prepared as above using un-patterned ITO coated glass (4 cm²) and avoiding the evaporation step. The counter electrode was prepared with chloroplatinic acid, H₂PtCl₆, in ethanol solution onto FTO glass and heating in an oven

at 450 °C for 30 min. A silicon spacer (50 μm thick) was used between the electrode and the counter electrode with a circular hollow space of area 0.26 cm^2 filled with the electrolyte solution. Alternatively, for electrodes replacing ZnO by PEDOT:PSS the spin coating step of PEDOT:PSS was carried out at 5500 rpm for 1 minute, film thickness of ~ 35 nm.

Device characterization.

Current density-voltage measurements of photovoltaic devices showed in Figure 1 were carried out by illumination with a 1.5G illumination source (100 mW cm^{-2}) using an Abet Sun 2000 Solar Simulator. The light intensity was adjusted with a calibrated Si solar cell. The photoelectrochemical characterization was performed in a three-electrode configuration, where a graphite bar and a Ag/Ag^+ (AgNO_3 0.1 M in acetonitrile) were, respectively, used as counterelectrode and as reference. The distance between working and counter electrodes was 1 cm approximately. The electrolyte was a 0.1 M tetrabutylammonium hexafluorophosphate solution in acetonitrile with a redox pair ferrocene (Fc/Fc^+ , 0.16 M) or benzoquinone (BZQ/BZQ^- , 0.2 M). The electrodes were illuminated through the substrate using a 300 W Xe lamp, where the light intensity was adjusted with a thermopile to 100 mW cm^{-2} . All potentials have been referred to the ferrocene redox potential: $E_{\text{Fc}/\text{Fc}^+} = E_{\text{Ag}/\text{Ag}^+} - 0.0716$. Capacitance-Voltage measurements were performed with a PGSTAT-30 Autolab potentiostat equipped with a frequency analyzer module, and were recorded by applying a small voltage perturbation (20 mV rms). Measurements were carried out under dark conditions at a frequency of 1000 Hz. External Quantum Efficiency (*EQE*) measurements were performed at short-circuit using a 150 W Xe lamp coupled with a monochromator controlled by a computer. The light intensity was measured using an optical power meter 70310 from Oriel Instruments where a Si photodiode was used to calibrate the system. Labelling

experiments were carried out with a homemade sealed photoelectrochemical cell, where an Ar stream ($\sim 12 \text{ mL min}^{-1}$) was constantly flowing through the cell. The electrode was immersed in the solution and illuminated through the electrolyte. The outlet gas was analyzed by an Agilent Technologies AG-490 gas chromatograph.

Continuous-wave photo-induced absorption spectra were performed in transmission geometry. A 560 nm laser diode served as the pump beam, modulated by a mechanical chopper at a frequency of 133 Hz. Transmission spectra are recorded using a probe beam from a Tungsten halogen lamp, focused on the sample by spherical mirrors in order to avoid chromatic aberrations. The transmitted light is dispersed with a monochromator and detected by a photodiode. The photoinduced variations of the transmission in the sample were recorded using a lock-in amplifier. All the differential spectra have been corrected for the photoluminescence and normalized by the transmission spectrum.

Acknowledgements

We acknowledge the financial support of the European Community through the Future and Emerging Technologies (FET) programme under the FP7, collaborative Project contract n° 309223 (PHOCS). MRA acknowledges contribution through EU project OLIMPIA, FP7-PEOPLE-212-ITN 316832 and by national grant Telethon – Italy, Grant N. GGP12033. We would like to thank Gene's Ink for the supply of ZnO nanoparticles.

Additional information

Electronic Supplementary Information (ESI) available: [Shuttered j-V curves of additional IFL/BHJ/redox couple configurations, zoom of the area of inversion of the

photocurrent in Figure 3, stability tests and labeling experiments]. See DOI: 10.1039/b000000x/

Competing financial interests: The authors declare no competing financial interests.

References

1. M. G. Walter, E. L. Warren, J. R. McKone, S. W. Boettcher, Q. Mi, E. A. Santori and N. S. Lewis, *Chemical Reviews*, 2010, **110**, 6446-6473.
2. M. Ni, M. K. H. Leung, D. Y. C. Leung and K. Sumathy, *Renewable & Sustainable Energy Reviews*, 2007, **11**, 401-425.
3. T. W. Hamann, *Dalton Transactions*, 2012, **41**, 7830-7834.
4. A. Tacca, L. Meda, G. Marra, A. Savoini, S. Caramori, V. Cristino, C. A. Bignozzi, V. G. Pedro, P. P. Boix, S. Gimenez and J. Bisquert, *Chemphyschem*, 2012, **13**, 3025-3034.
5. Y. Park, K. J. McDonald and K. S. Choi, *Chemical Society Reviews*, 2013, **42**, 2321-2337.
6. M. S. Prévot and K. Sivula, *The Journal of Physical Chemistry C*, 2013, **117**, 17879-17893.
7. N. S. Sariciftci, L. Smilowitz, A. J. Heeger and F. Wudl, *Science*, 1992, **258**, 1474-1476.
8. M. A. Green, K. Emery, Y. Hishikawa, W. Warta and E. D. Dunlop, *Prog Photovoltaics*, 2012, **20**, 12-20.
9. Z. He, C. Zhong, S. Su, M. Xu, H. Wu and Y. Cao, *Nature Photonics*, 2012, **6**, 591-595.
10. J. Danziger, J. P. Dodelet and N. R. Armstrong, *Chemistry of Materials*, 1991, **3**, 812-820.
11. V. Gautam, M. Bag and K. S. Narayan, *The Journal of Physical Chemistry Letters*, 2010, **1**, 3277-3282.
12. C. Janaky, N. R. de Tacconi, W. Chanmanee and K. Rajeshwar, *Journal of Physical Chemistry C*, 2012, **116**, 4234-4242.
13. E. Lanzarini, M. R. Antognazza, M. Biso, A. Ansaldo, L. Laudato, P. Bruno, P. Metrangolo, G. Resnati, D. Ricci and G. Lanzani, *The Journal of Physical Chemistry C*, 2012, **116**, 10944-10949.
14. G. Suppes, E. Ballard and S. Holdcroft, *Polymer Chemistry*, 2013, **4**, 5345-5350.
15. Z. F. Wang, P. Xiao, L. Qiao, X. Q. Meng, Y. H. Zhang, X. L. Li and F. Yang, *Physica B-Condensed Matter*, 2013, **419**, 51-56.

16. T. Yohannes, T. Solomon and O. Inganäs, *Synthetic Metals*, 1996, **82**, 215-220.
17. W. A. Gazotti, A. F. Nogueira, E. M. Giroto, M. C. Gallazzi and M. A. De Paoli, *Synthetic Metals*, 2000, **108**, 151-157.
18. A. Sergawie, T. Yohannes, S. Günes, H. Neugebauer and N. S. Sariciftci, *J. Braz. Chem. Soc.*, 2007, **18**, 1189-1193.
19. P. P. Boix, A. Guerrero, L. F. Marchesi, G. Garcia-Belmonte and J. Bisquert, *Advanced Energy Materials*, 2011, **1**, 1073-1078.
20. P. P. Boix, G. Garcia-Belmonte, U. Munecas, M. Neophytou, C. Waldauf and R. Pacios, *Applied Physics Letters*, 2009, **95**, 233302.
21. G. F. A. Dibb, M.-A. Muth, T. Kirchartz, S. Engmann, H. Hoppe, G. Gobsch, M. Thelakkat, N. Blouin, S. Tierney, M. Carrasco-Orozco, J. R. Durrant and J. Nelson, *Sci. Rep.*, 2013, **3**.
22. A. Guerrero, L. F. Marchesi, P. P. Boix, S. Ruiz-Raga, T. Ripolles-Sanchis, G. Garcia-Belmonte and J. Bisquert, *ACS Nano*, 2012, **6**, 3453-3460.
23. F. E. Osterloh, M. A. Holmes, L. L. Chang, A. J. Moule and J. Zhao, *Journal of Physical Chemistry C*, 2013, **117**, 26905-26913.
24. I. Mora-Sero, L. Bertoluzzi, V. Gonzalez-Pedro, S. Gimenez, F. Fabregat-Santiago, K. W. Kemp, E. H. Sargent and J. Bisquert, *Nature communications*, 2013, **4**.
25. R. A. Marcus, *The Journal of Chemical Physics*, 1956, **24**, 966-978.
26. R. A. Marcus, *Reviews of Modern Physics*, 1993, **65**, 599-610.
27. K. Ziemelis, A. Hussain, D. Bradley, R. Friend, J. Rühle and G. Wegner, *Physical review letters*, 1991, **66**, 2231.
28. R. Österbacka, C. An, X. Jiang and Z. Vardeny, *Science*, 2000, **287**, 839-842.
29. M. Antognazza, D. Ghezzi, D. Musitelli, M. Garbugli and G. Lanzani, *Applied Physics Letters*, 2009, **94**, 243501.
30. K. M. Noone, S. Subramaniyan, Q. Zhang, G. Cao, S. A. Jenekhe and D. S. Ginger, *The Journal of Physical Chemistry C*, 2011, **115**, 24403-24410.
31. K. M. Noone, E. Strein, N. C. Anderson, P.-T. Wu, S. A. Jenekhe and D. S. Ginger, *Nano letters*, 2010, **10**, 2635-2639.
32. X. Y. Chin, J. Yin, Z. Wang, M. Caironi and C. Soci, *Sci. Rep.*, 2014, **4**.
33. E. A. Santori, N. C. Strandwitz, R. L. Grimm, B. S. Brunschwig, H. A. Atwater and N. S. Lewis, *Energy & Environmental Science*, 2014.
34. F. Fabregat-Santiago, G. Garcia-Belmonte, I. Mora-Sero and J. Bisquert, *Phys. Chem. Chem. Phys.*, 2011, **13**, 9083-9118.
35. D. Ghezzi, M. R. Antognazza, R. Maccarone, S. Bellani, E. Lanzarini, N. Martino, M. Mete, G. Pertile, S. Bisti, G. Lanzani and F. Benfenati, *Nature Photonics*, 2013, **7**, 400-406.

36. T. S. Ripolles, A. Guerrero and G. Garcia-Belmonte, *Applied Physics Letters*, 2013, **103**, -.
37. A. M. Nardes, M. Kemerink, M. M. de Kok, E. Vinken, K. Maturova and R. A. J. Janssen, *Organic Electronics*, 2008, **9**, 727-734.
38. X. Jiang, F. L. Wong, M. K. Fung and S. T. Lee, *Applied Physics Letters*, 2003, **83**, 1875-1877.
39. A. J. Bard, M. Stratmann and S. Licht, eds., *Encyclopedia of Electrochemistry, Volume 6, Semiconductor Electrodes and Photoelectrochemistry*, Wiley-VCH, 2002.
40. J. Ajuria, I. Etxebarria, W. Cambarau, U. Munecas, R. Tena-Zaera, J. C. Jimeno and R. Pacios, *Energy & Environmental Science*, 2011, **4**, 453-458.
41. P. P. Boix, J. Ajuria, I. Etxebarria, R. Pacios, G. Garcia-Belmonte and J. Bisquert, *The Journal of Physical Chemistry Letters*, 2011, **2**, 407-411.
42. J. L. Dempsey, B. S. Brunshwig, J. R. Winkler and H. B. Gray, *Accounts of chemical research*, 2009, **42**, 1995-2004.
43. X. Hu, B. M. Cossairt, B. S. Brunshwig, N. S. Lewis and J. C. Peters, *Chemical communications*, 2005, 4723-4725.
44. C. N. Valdez, J. L. Dempsey, B. S. Brunshwig, J. R. Winkler and H. B. Gray, *Proceedings of the National Academy of Sciences*, 2012, **109**, 15589-15593.
45. A. Fihri, V. Artero, M. Razavet, C. Baffert, W. Leibl and M. Fontecave, *Angewandte Chemie*, 2008, **120**, 574-577.
46. M. Razavet, V. Artero and M. Fontecave, *Inorganic chemistry*, 2005, **44**, 4786-4795.